Conformations of Polyaniline Molecules Adsorbed on Au(111) Probed by in Situ STM and ex Situ XPS and NEXAFS

YiHui Lee,[†] ChinZen Chang,[†] ShuehLin Yau,*,[†,‡] LiangJen Fan,*,[§] YawWen Yang,[§] LiangYueh Ou Yang,[||] and Kingo Itaya[||]

Department of Chemistry, National Central University, Zhongli, Taiwan 320, ROC, Department of Chemistry, Dalian University of Technology, No. 2 Linggong Road, Ganjinzi District, Dalian City, Liaoning Province, PRC 116024, National Synchrotron Radiation Research Center, 101 Hsin Ann Road, Hsinchu Science Park, Hsinchu, Taiwan 30076, ROC, and Department of Applied Chemistry, Graduate School of Engineering, Tohoku University, 6-6-07Aoba, Sendai 980-8579, Japan

Received November 26, 2008; E-mail: yau6017@ncu.edu.tw

Abstract: In situ scanning tunneling microscopy (STM), X-ray photoelectron spectroscopy (XPS), and near edge X-ray absorption fine structure (NEXAFS) have been used to examine the conformation of a monolayer of polyaniline (PAN) molecules produced on a Au(111) single-crystal electrode by anodization at 1.0 V [vs reversible hydrogen electrode (RHE)] in 0.10 M H_2SO_4 containing 0.030 M aniline. The as-produced PAN molecules took on a well-defined linear conformation stretching for 500 Å or more, as shown by in situ and ex situ STM. The XPS and NEXAFS results indicated that the linear PAN seen at 1.0 V assumed the form of an emeraldine salt made of PAN chains and (bi)sulfate anions. Shifting the potential from 1.0 to 0.7 V altered the shape of the PAN molecules from straight to crooked, which was ascribed to restructuring of the Au(111) electrified interface on the basis of voltammetric and XPS results. In situ STM showed that further decreasing the potential to 0.5 V transformed the crooked PAN threads into a mostly linear form again, with preferential alignment and formation of some locally ordered structures. PAN molecules could be reduced from emeraldine to leucoemeraldine as the potential was decreased to 0.2 V or less. In situ STM showed that the fully reduced PAN molecules were straight but mysteriously shortened to ~50 Å in length. The conformation of PAN did not recuperate when the potential was shifted positively to 1.0 V.

Introduction

Polyaniline (PAN), although known for more than a century, continues to draw interest from a wide spectrum of research disciplines ranging from electrochemistry to material science.[1−3] The renewed research activity on PAN is fueled by the development of new characterization methods and procedures to harness nanomaterials that are potentially useful in fabricating sensors, batteries, and probes in biotechnology.[4−15] Probing the size, molecular structure, and conformation has been an important task because these microscopic characteristics can influence the macroscopic properties of PAN. From the perspective of interfacial structure, the adsorption of organic molecules on substrates has been the key to unraveling many interfacial processes. For example, a thorough understanding of molecular orientation at an electrode can yield a tangible model that describes the kinetics of electron transport across an interface, as illustrated by theoretical and experimental studies.[16,17] Although the adsorption of organic molecules on metallic substrates such as copper, silver, gold, platinum, and so forth has been extensively examined, the studies of the adsorption of polymers on well-defined substrates are limited. Only a few studies address how PAN molecules are adsorbed on electrodes with an ordered atomic arrangement.[18]

[†] National Central University.
[‡] Dalian University of Technology.
[§] National Synchrotron Radiation Research Center.
[||] Tohoku University.

(1) Huang, W. S.; Humphrey, B. D.; MacDiarmid, A. G. *J. Chem. Soc., Faraday Trans. 1* **1986**, *82*, 2385–2400.
(2) Orata, D.; Buttry, D. A. *J. Am. Chem. Soc.* **1987**, *109*, 3574–3581.
(3) Takei, T.; Kobayashi, Y.; Hata, H.; Yonesaki, Y.; Kumada, N.; Kinomura, N.; Mallouk, T. E. *J. Am. Chem. Soc.* **2006**, *128*, 16634–16640.
(4) Chao, S.; Wrighton, M. S. *J. Am. Chem. Soc.* **1987**, *109*, 6627–6631.
(5) Rozsnyai, L. F.; Wrighton, M. S. *J. Am. Chem. Soc.* **1994**, *116*, 5993–5994.
(6) Liu, W.; Cholli, A. L.; Nagarajan, R.; Kumar, J.; Tripathy, S.; Bruno, F. F.; Samuelson, L. *J. Am. Chem. Soc.* **1999**, *121*, 11345–11355.
(7) Raitman, O. A.; Katz, E.; Buckmann, A. F.; Willner, I. *J. Am. Chem. Soc.* **2002**, *124*, 6487–6496.
(8) Zhang, J.; Barker, A. L.; Mandler, D.; Unwin, P. R. *J. Am. Chem. Soc.* **2003**, *125*, 9312–9313.
(9) Huang, J.; Virji, S.; Weiller, B. H.; Kaner, R. B. *J. Am. Chem. Soc.* **2003**, *125*, 314–315.
(10) Thiyagarajan, M.; Samuelson, L. A.; Kumar, J.; Cholli, A. L. *J. Am. Chem. Soc.* **2003**, *125*, 11502–11503.

(11) Carswell, A. D. W.; O'Rear, E. A.; Grady, B. P. *J. Am. Chem. Soc.* **2003**, *125*, 14793–14800.
(12) Zhang, X.; Goux, W. J.; Manohar, S. K. *J. Am. Chem. Soc.* **2004**, *126*, 4502–4503.
(13) Li, W.; Wang, H. L. *J. Am. Chem. Soc.* **2004**, *126*, 2278–2279.
(14) Ma, Y.; Zhang, J.; Zhang, G.; He, H. *J. Am. Chem. Soc.* **2004**, *126*, 7097–7101.
(15) Ma, Y.; Ali, S. R.; Wang, L.; Chiu, P. L.; Mendelsohn, R.; He, H. *J. Am. Chem. Soc.* **2006**, *128*, 12064–12065.
(16) Kornilovitch, P. E.; Bratkovsky, A. M. *Phys. Rev. B* **2001**, *64*, 195413.
(17) He, H.; Zhu, J.; Tao, N. J.; Nagahara, L. A.; Amlani, I.; Tsui, R. *J. Am. Chem. Soc.* **2001**, *123*, 7730–7731.
(18) Xu, B.; Jaewu, C.; Dowben, P. A. *J. Vac. Sci. Technol., A* **2002**, *20*, 741–743.

10.1021/ja809263y CCC: $40.75 © 2009 American Chemical Society

Scanning tunneling microscopy (STM), with its renowned subnanometer resolution capability, has been used to probe the organization of polymeric materials in vacuum and in electrochemistry.[19−24] In previous work, we took advantage of this technique to gain molecular insights into the adsorption and polymerization of aniline molecules on Au(111) under electrochemical potential control.[25] On Au(111), aniline molecules were found to adsorb in highly ordered arrays and polymerize into PAN with well-defined linear molecular conformations stretching for 500 Å or more in some specific directions. These characteristics of PAN are thought to stem from a special lateral arrangement of aniline monomers and coadsorbed bisulfate anions. In stark contrast, polyaniline molecules produced on a rough gold electrode were found to be poorly defined in shape.[25]

The rich and yet intricate electrochemistry of PAN is well-documented.[26−33] However, it is not yet clear how the molecular structure and conformation of PAN vary with potential. PAN molecules can take on three oxidation states, including leucoemeraldine (the fully reduced form), emeraldine (the half-oxidized form), and pernigraldine (the fully oxidized form).[1] Among these, only the half-oxidized state, in the form of an emeraldine salt made of PAN chains and anions such as (bi)sulfate, perchlorate, and chloride, has been shown to be conductive. The other two states, which prevail at negative and positive potentials, respectively, are neutralized by exclusion or inclusion of cations or anions in the film.[2,34] The packing habit of PAN, which could be important for its physical properties, has been examined using X-ray diffraction techniques and theoretical calculations.[35,36] The arrangement of PAN molecules in films produced electrochemically on an electrode is unclear.

In addition to the STM imaging technique, we have used X-ray photoelectron spectroscopy (XPS) and near edge X-ray absorption fine structure (NEXAFS) spectroscopy to identify the chemical nature of PAN formed under the conditions the same as those for STM. Results obtained here showed that at potentials as positive as 1.0 V [vs reversible hydrogen electrode (RHE)], PAN molecules were formed on Au(111) predominantly as the emeraldine salt.[37,38] Molecular-resolution STM imaging indicated drastic changes in PAN conformation as the potential was varied.

Experimental Section

The Au(111) single-crystal electrode used for cyclic voltammetry (CV) and STM experiments was made by melting a Au wire ($\phi = 0.8$ mm) with a hydrogen torch, as reported earlier.[39,40] All of the electrochemical experiments were performed with the conventional hanging meniscus method in a three-electrode cell. The RHE and a Pt wire acted as the reference and counter electrodes, respectively. A CHI 703 potentiostat was used. The supporting electrolyte was typically 0.1 M H_2SO_4 containing 0.030 M aniline. Ultrapure H_2SO_4 was purchased from Merck (Darmstadt, DFG), while aniline was obtained from Aldrich (St. Louis, MO) and used after distillation. Triple-distilled Millipore water (resistivity 18.3 MΩ) was used to prepare all of the solutions.

STM in this study was performed using a Nanoscope E (Digital Instruments, Santa Barbara, CA) with a single-tube scanner (high-resolution A-head, maximal scan area ∼6000 Å²). Tungsten tips ($\phi = 0.3$ mm) prepared by electrochemical etching in 2 M KOH were used throughout this study. Each tip was water-rinsed, dried by acetone washing, and finally painted with nail polish for insulation. The use of STM in studying electrified interfaces has been reviewed.[19,21]

The substrates used for ex situ XPS and NEXAFS experiments were borosilica slides coated with 2000 Å thick gold (Arrandee, Werther, DFG). The substrate was cleaned by annealing with a butane flame followed by quenching in triple-distilled Millipore water. This process yielded (111) grains stretching for hundreds of nanometers. The as-prepared gold substrate was then transferred to an electrochemical cell, which housed the RHE and a Pt counter electrode. The electrolyte was 1.0 M H_2SO_4 containing 0.030 M aniline, from which aniline molecules were deposited and electropolymerized onto the gold electrode. The thickness of the PAN film was controlled by holding the potential at 1.0 V for a predetermined period of time. The sample was then pulled out of the solution under potential control and transferred onto the STM stage. The sample was dried and imaged in a dry nitrogen environment. Finally, the sample was transferred into a UHV chamber, where the XPS and NEXAFS experiments were performed. Well-defined linear PAN chains, as also seen by in situ STM, were observed using molecular-resolution STM imaging under nitrogen. This result suggests that the X-ray results, despite being obtained ex situ, could represent the interfacial structure of PAN/Au(111). A typical ex situ STM image is shown in the Supporting Information.

XPS and NEXAFS experiments were performed at a UHV end station attached to the BL24A wide-range spherical grating beamline at the NSRRC. The end station housed a differentially pumped sputter-ion gun for sample cleaning, a SPEC Phoiboss150 energy analyzer for XPS, a multichannel plate (MCP) detector for NEXAFS, and a load−lock sample transfer mechanism. The XPS binding energy scale was referenced to the bulk Au 4f$_{7/2}$ core level located at 84.00 eV relative to Fermi level. The XPS used a photon energies of 630 and 500 eV, respectively, for the survey scan and high-resolution N(1s) and S(2p) scans. The combined-instrument energy resolution for the high-resolution scans was set at 0.3 eV.

Polarization-dependent NEXAFS measurements were performed by the partial electron yield (PEY) method with an MCP detector set at a retarding voltage of −150 V at various X-ray incident angles (θ) from 90° (normal incidence) to 20° (grazing incidence). The NEXAFS photon energy scale for the carbon K-edge was calibrated

(19) Itaya, K. *Prog. Surf. Sci.* **1998**, *58*, 121–247.
(20) Gewirth, A. A.; Niece, B. K. *Chem. Rev.* **1997**, *97*, 1129–1162.
(21) Magnussen, O. M. *Chem. Rev.* **2002**, *102*, 679–726.
(22) Mena-Osteritz, E.; Meyer, A.; Langeveld-Voss, B. M. W.; Janssen, R. A. J.; Meijer, E. W.; Bäuerle, P. *Angew. Chem., Int. Ed.* **2000**, *39*, 2679–2684.
(23) Sakaguchi, H.; Matsumura, H.; Gong, H.; Abouelwafa, A. M. *Science* **2005**, *310*, 1002–1006.
(24) Akai-Kasaya, M.; Shimizu, K.; Watanabe, Y.; Saito, A.; Aono, M.; Kuwahara, Y. *Phys. Rev. Lett.* **2003**, *91*, 255501.
(25) Yang, L. Y. O.; Chang, C.; Liu, S.; Wu, C.; Yau, S. L. *J. Am. Chem. Soc.* **2007**, *129*, 8076–8077.
(26) David, E. S.; Park, S.-M. *J. Electrochem. Soc.* **1988**, *135*, 2497–2502.
(27) David, E. S.; Park, S.-M. *J. Electrochem. Soc.* **1989**, *136*, 427–433.
(28) Cho, S. H.; Kim, D.; Park, S.-M. *Electrochim. Acta* **2008**, *53*, 3820–3827.
(29) Chen, Y.; Wang, X. H.; Li, J.; Lu, J. L.; Wang, F. S. *Electrochim. Acta* **2007**, *52*, 5392–5399.
(30) Xu, K.; Zhu, L.; Wu, Y.; Tang, H. *Electrochim. Acta* **2006**, *51*, 3986–3992.
(31) Palys, B.; Celuch, P. *Electrochim. Acta* **2006**, *51*, 4115–4124.
(32) Gupta, V.; Miura, N. *Electrochim. Acta* **2006**, *52*, 1721–1726.
(33) Ghanbari, K.; Mousavi, M. F.; Shamsipur, M. *Electrochim. Acta* **2006**, *52*, 1514–1522.
(34) Shin-Jung, C.; Su-Moon, P. *J. Electrochem. Soc.* **2002**, *149*, E26−E34.
(35) Pouget, J. P.; Jozefowicz, M. E.; Epstein, A. J.; Tang, X.; MacDiarmid, A. G. *Macromolecules* **1991**, *24*, 779–789.
(36) Ginder, J. M.; Epstein, A. J. *Phys. Rev. B* **1990**, *41*, 10674–10685.
(37) Shim, Y.-B.; Won, M.-S.; Park, S.-M. *J. Electrochem. Soc.* **1990**, *137*, 538–544.
(38) Cui, C. Q.; Ong, L. H.; Tan, T. C.; Lee, J. Y. *Synth. Met.* **1993**, *58*, 147–160.
(39) Hamelin, A. *J. Electroanal. Chem.* **1996**, *407*, 1–11.
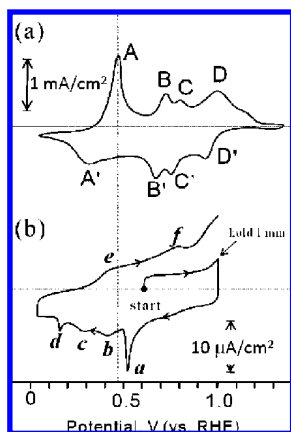(40) Chang, C.-C.; Yau, S.-L.; Tu, J.-W.; Yang, J.-S. *Surf. Sci.* **2003**, *523*, 59–67.

Figure 1. Cyclic voltammograms recorded at 50 mV/s with a Au(111) electrode in 0.1 M H$_2$SO$_4$ containing 0.03 M aniline. The results shown in (a) are the 40th and 41st scans of continuous potential cycling between 0.05 and 1.3 V. The potential program for (b) was started at 0.6 V, scanned positively to 1.0 V, held at 1.0 V for 1 min, scanned negatively to 0.05 V, and reversed.

Figure 2. High-resolution N(1s) XPS spectra together with the least-squares fitting results for a 3 Å PAN film on Au(111) at (a, b) 1.0 and (c, d) 0.5 V detected (a, c) in normal emission geometry with a takeoff angle of 90° and (b, d) grazing emission geometry with a takeoff angle of 30°.

against the intense 1s → π* transition of highly oriented pyrolytic graphite (HOPG) located at 285.38 eV. The spectra were first normalized to the photon flux to give the so-called Io-normalized spectrum, with the flux obtained by measuring the ionization current of argon gas in a specially designed gas ionization chamber situated in front of the sample.[41] The X-ray absorption features of the substrate were eliminated by dividing the Io-normalized PEY spectrum of a PAN-covered Au(111) surface by the Io-normalized PEY spectrum of a clean Au(111) surface, where the spectra were measured separately but under the same photon incidence conditions. All of the spectra presented were identically treated.

Results and Discussion

Cyclic Voltammetry. PAN can exist in three possible oxidation states, namely, leucoemeraldine, emeraldine, and pernigraldine, which are successively reached as the potential is made more and more positive in acidic solutions.[1,2,26,34,38,42] Cyclic voltammograms recorded at 50 mV/s with a Au(111) electrode in 0.1 M H$_2$SO$_4$ containing 0.03 M aniline are shown in Figure 1. When the potential was cycled continuously between 1.3 and 0.05 V, the current density in the profile grew with the number of cycles. Figure 1a shows the 40th and 41st scans, after a thick PAN film had already been produced there. Four pairs of peaks are evident, which include those associated with the redox of PAN molecules (A/A′ and D/D′) and those due to the redox of benzoquinone and aminoquinone species (B/B′ and C/C′), which are produced by the degradation of PAN at E > 1.1 V.[42−44]

To examine the redox chemistry of a thin PAN film on Au(111), we conducted voltammetry by sweeping the potential from the open-circuit potential (∼0.6 V) to 1.0 V. The potential was then held at 1.0 V for 1 min to allow the deposition of roughly a bilayer of PAN molecules on Au(111). This was followed by sweeping the potential negatively from 1.0 to 0.05 V at 50 mV/s. The resultant j−E profile (Figure 1b) was essentially featureless until 0.52 V, where a sharp peak emerged, followed by two broad peaks near 0.4 and 0.3 V and a somewhat sharper peak at 0.17 V. As evidenced by the different morphologies of the curves in Figure 1a,b, the thin PAN film
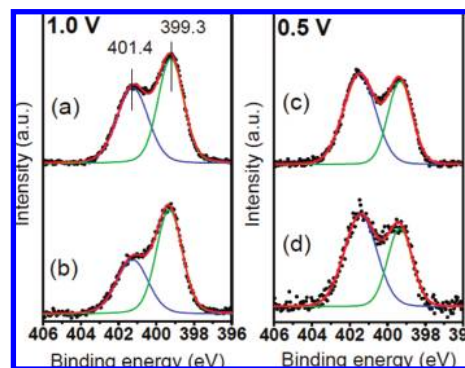
exhibited electrochemistry very different from that of the thick PAN film. The most pronounced reduction peak seen in Figure 1b (*a* at 0.52 V) had a peak current density of 10 μA/cm^2. The sharpness of this peak suggests that it is associated with some surface processes. Since it is located at a potential 0.33 V more negative than that for the reduction of pernigraldine to emeraldine seen for a thick PAN film (A/A′ in Figure 1a), the reduction peak *a* is unlikely to be associated with this reduction reaction. It is worth mentioning that the dimer and tetramer of aniline produce redox features at potentials nearly the same as that of extended polyaniline.[45]

The XPS results acquired with samples immersed at 1.0 and 0.5 V indicate that the PAN molecules were chemically identical. In other words, the PAN molecules were not reduced in this potential range. Thus, the most distinct feature *a* in the CV profile (Figure 1b) could be a charging event involving restructuring of the electric double layer of the Au(111) electrode. This view is line with STM results showing dramatic changes of the conformations of PAN in an irreversible manner (see below). The redox properties of the thin PAN film deposited on the metal electrode thus differ from those of a thick PAN film (Figure 1a). It appears that although PAN could be oxidized electrochemically at 1.0 V, it was reduced to the half-oxidized emeraldine when reacting with aniline monomers during polymerization.[37,38]

The nature of those reduction peaks appearing at potentials more negative than 0.52 V is not clear, partly because the Au(111) sample was not stable toward immersion and transfer into the vacuum environment. Reduction of emeraldine to leucoemeraldine could occur at E < 0.15 V, resulting in a dramatic decrease in the charging current because the fully reduced form of PAN conducts poorly.[2] The thin PAN film could be oxidized at 0.42 V, giving rise to a weak peak *e*. The oxidation peak *f* at 0.75 V could be associated with the reverse reaction of peak *a*, and the lack of reversibility of the **a/f** couple might derive from the difficulty of reverting the structure of PAN.

XPS and NEXAFS. The high-resolution N(1s) XPS spectra for PAN/Au(111) samples immersed at 1.0 and 0.5 V are shown in Figure 2; each reveals two distinct peaks at 399.3 and 401.4 eV. These features are ascribed to benzenoid amine and nitrogen cationic radical, respectively, as reported by others.[46] The relative intensities of these two peaks are almost identical, which

(41) Fan, L.-J. F.; Yang, Y.-W.; Lee, K. *AIP Conf. Proc.* **2007**, *882*, 920.
(42) Yang, H.; Bard, A. J. *J. Electroanal. Chem.* **1992**, *339*, 423–449.
(43) David, E. S.; Park, S.-M. *J. Electrochem. Soc.* **1988**, *135*, 2254–2262.
(44) Zhang, A. Q.; Cui, C. Q.; Lee, J. Y. *Synth. Met.* **1995**, *72*, 217–223.

(45) Shacklette, L. W.; Wolf, J. F.; Gould, S.; Baughman, R. H. *J. Chem. Phys.* **1988**, *88*, 3955–3961.
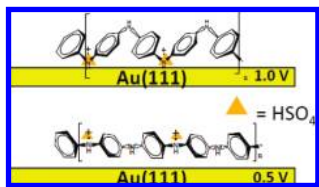
Figure 3. Schematic presentation of the relative positions of polyaniline and coadsorbed bisulfate ion on Au(111) prepared at 1.0 and 0.5 V.

implies that both samples were essentially emeraldine salts, the half-oxidized form of PAN. If PAN were oxidized to pernigraldine at 1.0 V, the XPS spectra should have shown a single N(1s) peak at 398.4 eV (quinonoid imine) or a pair of peaks at 389.4 (quinonoid imine) and 402.5 eV (protonated quinonoid imine) due to the fully oxidized form. In fact, none of these features has ever been observed for PAN samples prepared by anodization at 1.0 V.

As Figure 2 shows, the XPS spectrum for the 1.0 V sample contains less radical cation at 401.4 eV than benzenoid amine at 399.3 eV. As the potential is changed from 1.0 to 0.5 V, one might expect more of the reduced benzenoid amine at 399.3 eV. However, this is opposite to what was observed at 0.5 V, as the XPS signal at 399.3 eV for benzenoid amine instead became smaller than that at 1.0 V. It is likely that PAN admolecules changed their conformation at 0.5 V in a way that raised the nitrogen radical cation to a higher plane than that of 1.0 V, resulting in a larger signal at 401.4 eV.

To further scrutinize the structures of the PAN/Au(111) interface, we used angle-dependent XPS to probe the relative positions of species contained in the PAN films prepared at 1.0 and 0.5 V. XPS spectra were collected at two emission angles, the normal and grazing emission angles (90 and 30° from the surface, respectively). The latter measurement is more sensitive to chemical species located farther away from the Au(111) electrode. At 1.0 V, the signal at 401.4 eV due to the radical cation was reduced significantly at the grazing angle, while that at 0.5 V remained unchanged. These results show unambiguously that benzenoid amine groups were located farther away from the Au(111) electrode than cationic nitrogen radicals at 1.0 V, whereas at 0.5 V the radical cation and benzenoid amine were distributed uniformly. The location of the adsorbed (bi)sulfate counteranion at the Au(111) electrode was similarly examined. At 1.0 V, the ratio of the peak areas for the N(1s) and S(2p) peak was 2.62 and 2.5 at normal and grazing emission, respectively, whereas they were 2.4 and 4.06, respectively, for Au(111) at 0.5 V. These results indicate that the coadsorbed (bi)sulfate anions repositioned themselves in response to the modulation of the potential, as illustrated by the model shown in Figure 3. This trend is thought to reflect electrostatic interaction between the charged species and the Au(111) electrode.

To further analyze the structure of the PAN, we used polarization-dependent carbon K-edge NEXAFS to elucidate the tilt angles as well as the electronic structure of the PAN. In NEXAFS spectroscopy, tunable and linearly polarized soft X-rays are absorbed, causing resonant excitations of core electrons to unoccupied molecular orbitals such as π^* or σ^*. Figure 4 shows the NEXAFS spectra acquired at 1.0 and 0.5 V, respectively, for Au(111) coated with 3 Å of PAN. A number

(46) Guay, D.; Stewart-Ornstein, J.; Zhang, X.; Hitchcock, A. P. *Anal. Chem.* **2005**, *77*, 3479–3487.
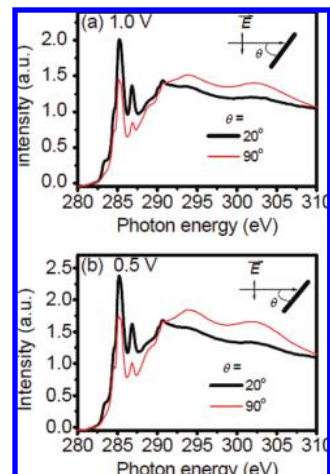

Figure 4. Selective polarization-dependent carbon K-edge NEXAFS spectra for 3 Å PAN prepared at (a) 1.0 and (b) 0.5 V at normal (red) and grazing (black) photon incidence angles.

of peaks appear between 283 and 310 eV, which agree with the results reported by Guay et al.[46] Among these, the peaks at 283.4, 285.2, and 286.8 eV are associated with C 1s(C=C) → $\pi^*_{C=C}$ transitions in the quinonoid ring, the C 1s(C–H) → π^*_{ring} transition of the benzenoid ring, and the C 1s(C–N) → π^*_{ring} transition, respectively.[46] Two broad peaks at higher binding energies of 294 and 302 eV correspond to σ^*_{CC} states. The morphologies of these two spectra are essentially identical, indicating that the PAN molecules resulting from immersion at 0.5 and 1.0 V are chemically identical. This view agrees with that derived from the XPS results described above. When compared with results obtained using much thicker PAN films,[46] our present spectra show that (1) the peak position of the C 1s(C=C) → $\pi^*_{C=C}$ transitions in the quinonoid ring is shifted 0.4 eV lower and (2) a shoulder on the C 1s(C–H) → π^*_{ring} transition of the benzenoid ring appears at 284.5 eV, and its intensity diminishes with increasing PAN thickness. We therefore assign the shoulder as the C 1s(C–H) → π^*_{ring} transition of the benzenoid ring for the first PAN layer on Au(111). These peak shifts seen for the quinonoid and benzenoid rings imply that the PAN molecules interacted strongly with the Au(111) surface, which is in line with results showing that the energy of unoccupied orbitals of the free molecule may differ from the those for the adsorbed one.[47]

The first three π^* peaks are the most intense ones at a grazing photon incidence angle of 20°, indicating that both the benzenoid and quinonoid rings in the PAN molecule were tilted by 55° or less with respect to the Au(111) surface. We followed the procedure outlined by Stohr[48] to quantitatively assess those peaks in the spectra shown in Figure 4. The tilt angles enclosed by the ring plane of the quinonoid ring and the Au(111) surface were determined to be ∼37 and 45° at 1.0 and 0.5 V, respectively, whereas they were ∼50° for the benzenoid ring in both cases. The difference in the tilt angles for the benzenoid and quinonoid rings reflects the zigzag conformation of PAN molecules on Au(111). At 1.0 V, the quinonoid ring of the PAN molecule leaned toward the Au(111) surface, possibly because it interacted with the gold electrode mainly via the quinonoid imine functional group. This view is consistent with the XPS

(47) Käfer, D.; Witte, G. *Chem. Phys. Lett.* **2007**, *442*, 376–383.
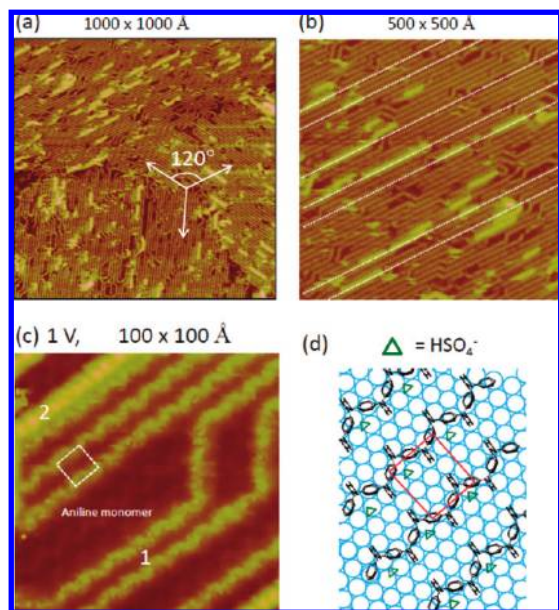(48) Stohr, J. *NEXAFS Spetroscopy*; Springer Series in Surface Sciences, Vol. 25; Springer: Berlin, 1992.

Figure 5. In situ STM images obtained with Au(111) at 1.0 V in 0.1 M H_2SO_4 containing 0.03 M aniline. Three rotational domains of PAN molecules are seen in (a), and the higher resolution scan in (b) shows the formation of multilayer PAN. The molecular-resolution scan in (c) discloses the internal molecular structure. A corresponding real-space model is shown in (d), with green triangles representing bisulfate anions bridging PAN molecules and the Au(111) substrate.

results, which also showed that the radical cation was close to the Au(111) surface.

Linear Polyaniline Formed at 1.0 V on Au(111). The structure of the aniline overlayer and the initial electropolymerization process on Au(111) were reported earlier.[25] In this study, we focused on the conformation of PAN admolecules as a function of electrochemical potential. Given the complexity and information from STM and XPS, we could only account for the most prominent PAN structures. Careful control of the potential was needed because overpotential dominated the rate of oxidation of aniline and the subsequent polymerization on Au(111). We noted that a change in potential from 0.90 to 1.0 V was enough to transform aniline monomers arranging in a $(3 \times 2\sqrt{3})$rect structure into linear PAN molecules, which were imaged as straight lines bulging by 3.5 Å (Figure 5a). It appears that some aniline admolecules were oxidized to radical cations, which reacted quickly with their neighbors to produce polyaniline molecules.[26]

This polymerization process could yield sub- to multilayer PAN films, depending on how long the potential was held at 1.0 V. The intensity of the PAN molecules in the STM image reflects their heights on Au(111). High-quality STM was possible on a four-layer-thick PAN as long as the feedback current was set at less than 1 nA. The as-formed PAN chains grew easily to 300 Å in length and could reach 1000 Å, all depending on the quality of the Au(111) surface. The key to preparing long and straight PAN molecules lies in making a well-ordered $(3 \times 2\sqrt{3})$rect aniline structure at 0.90 V prior to polymerization. These STM results indicate that anodization was effective in producing linear PAN molecular wires, although defects of 120° (bent or hairpinlike fold) were always present.

The as-produced PAN admolecules were always aligned in three specific directions that correspond to the <110> directions of Au(111), according to the STM results. Two neighboring PAN chains were uniformly spaced by 10.4 Å, which equals

the length of the $2\sqrt{3}$ unit vector of the $(3 \times 2\sqrt{3})$rect aniline structure. This intermolecular spacing persisted as the PAN film grew thicker. The white dotted lines marked in Figure 5b are intended to show that PAN chains in the upper tiers were perched on rather than between the chains on the lower planes. This arrangement may be classified as molecular epitaxy, which can be likened to layers of bricks used in constructing buildings. PAN chains lying in the lower planes acted as a template that guided the subsequent growth of another layer of PAN. It should be noted that similar epitaxial organization of polymers was noted previously for poly(3-dodecylthiophene) deposited on HOPG.[49]

The difference between the heights of two PAN layers was ~3.5 Å, which equals the thickness of the π-electron cloud of a benzene molecule.[50] This result is also consistent with a theoretical study on the structure of PAN showing that PAN can stack with the electron-rich benzenoid rings sitting atop electron-deficient quinonoid rings. The height difference of 3.5 Å has previously been reported.[51] Compared with the 0.75 Å corrugation seen for aniline monomer in the STM, the 3.5 Å corrugation height seen for PAN is phenomenal. To our knowledge, it is difficult to use STM to image multilayered aromatic admolecules, possibly because of the lack of sufficient conductivity and the high mobility of the adsorbate. For STM imaging of multilayered aromatics, the corrugation height between different layers hardly reflects their physical dimensions.[52] The present STM results are intriguing on these grounds, in that the imaging was stable, reproducible, and definitive up to a thickness of four molecular layers. All of these results attest to the idea that the PAN film seen here is metallic. A quantitative description of the conductivity of this well-defined PAN film awaits further investigation.

Molecular-resolution STM imaging was used to examine the internal molecular structures of PAN admolecules. Figure 5c shows a typical STM image, in which each PAN molecule was imaged as a chain of oval protrusions linked back-to-back along the main axis of the Au(111) substrate. The oval protrusions are attributed to the aromatic rings in a PAN molecule: two neighboring rings separated from each other by 4.5 Å. Two nearest-neighbor PAN chains were 10.4 Å apart, which corresponds to the length of a $2\sqrt{3}$ unit vector. Thus, the PAN admolecules were commensurate with the Au(111) substrate, as the model in Figure 5d portrays. According to the XPS results described above, the linear chains of PAN seen at 1.0 V were emeraldine salt, comprising aniline monomers and bisulfate anions.[35] The coadsorbed (bi)sulfate anions were difficult to see with the STM, possibly because they lay at a lower plane than the PAN and the imaging parameters used here were not proper for tunneling through the bisulfate species. The adsorption of (bi)sulfate anion at gold electrodes has been extensively examined.[53,54]

Transformation from Straight to Crooked PAN Molecules at 0.7 V. An STM imaging experiment to explore potential-induced changes in PAN conformation started by producing a

(49) Scifo, L.; Dubois, M.; Brun, M.; Rannou, P.; Latil, S.; Rubio, A.; Grévin, B. *Nano Lett.* **2006**, *6*, 1711–1718.

(50) Carey, F. A. *Organic Chemistry*, 2nd ed.; McGraw-Hill, Inc: New York, 1992.

(51) Ivanova, A.; Madjarova, G.; Tadjer, A.; Gospodinova, N. *Int. J. Quantum Chem.* **2006**, *106*, 1383–1395.

(52) Joo, H. K.; Zhu, X. Y. *Appl. Phys. Lett.* **2003**, *82*, 3248–3250.

(53) Magnussen, O. M.; Hageböck, J.; Hotlos, J.; Behm, R. J. *Faraday Discuss.* **1992**, *94*, 329–338.

(54) Edens, G. J.; Gao, X.; Weaver, M. J. *J. Electroanal. Chem.* **1994**, *375*, 357–366.
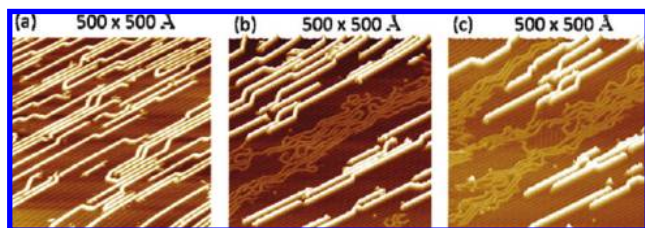
Figure 6. In situ STM images showing changes of molecular conformation resulting from a switch of potential from 0.95 to 0.7 V. The time lapses from (a) to (b) and then to (c) were 8 and 11 min, respectively. Straight PAN chains turned crooked gradually.
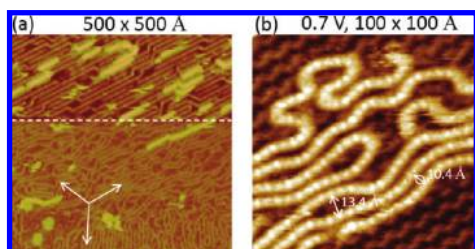

Figure 7. (a) In situ STM images showing the instantaneous changes of molecular conformation as the potential was stepped from 1.0 to 0.6 V. (b) Molecular-resolution STM scan revealing the internal molecular arrangement of PAN molecules. The arrows in (a) mark the direction of the main axes of the Au(111) substrate. The ordered pattern seen in the background is the $(3 \times 2\sqrt{3})$rect aniline adlattice.

half-monolayer of PAN admolecules on Au(111) when the potential was held at 0.95 V for 2 min. PAN chains spanning 500 Å along with the $(3 \times 2\sqrt{3})$rect aniline array are seen in Figure 6a. Switching the potential from 0.95 to 0.7 V caused a dramatic change in the PAN conformation from straight chains to crooked threads. This structural transformation commenced at the ends of PAN chain and crept into the chain, as seen in Figure 6b,c. PAN molecules became substantially (-2.7 Å) lower as they turned crooked. This sudden drop in intensity seen simultaneously with the change of conformation could result from different electronic properties or different adsorption configurations of PAN molecules at different potentials. Spectroscopic STM could be one of the ways to resolve this issue, as illustrated by others.[49] Crooked threads continued to thrive over time at the expense of linear PAN chains. Although the $(3 \times 2\sqrt{3})$rect aniline structure continued to persist in the images, it was unable to regulate the orientation of the PAN chains. Crooked PAN molecules could get longer with time, suggesting that short PAN chains could have drifted on the surface until they were devoured by larger ones.

To ensure that the conformational changes seen in Figure 6 were indeed caused by an alternation of potential and to see how fast the change would occur, we acquired a composite STM image (Figure 7a) by switching the potential abruptly from 1.0 to 0.6 V as the tip was rastering downward to one-third of the frame. Initially linear PAN chains seen in the upper third of the frame turned crooked rapidly upon this shift of potential. This is not an imaging artifact because changing the potential of the tip would not produce this kind of result. Neither did it come from some sort of redox process, because as dramatically as it appeared in the STM, this process should have registered in the voltammogram. Despite the poorly defined molecular shape, PAN molecules were still long and independent entities, indicating that the PAN backbone remained intact and without cross-links. Switching the potential back to 0.95 V could uncurl
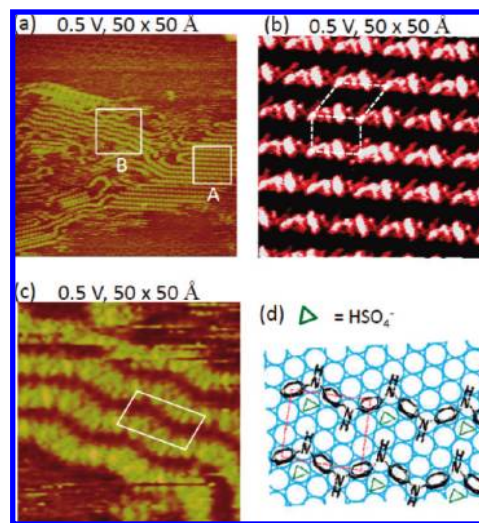

Figure 8. In situ STM images showing ordered PAN adlattices formed on Au(111) at 0.5 V in 0.1 M H_2SO_4 containing 0.03 M aniline. PAN molecules generally registered with the Au(111) substrate, forming $(3 \times 2\sqrt{3})$ and $(2\sqrt{3} \times 2\sqrt{3})$ unit cells in domain **A** and $(2\sqrt{3} \times \sqrt{43})$ in domain **B**. The structure of domain **A** seen in (b) is represented by the model shown in (d). The locally ordered array seen at the upper end of (a) is due to unknown species produced by the decomposition of PAN.

the PAN molecules, but the degree of linearity was not as good as that observed on the pristine Au(111) surface.

The internal molecular structure of crooked PAN threads was also discerned by a high-resolution scan, as Figure 7b illustrates. Each PAN molecule was again imaged as a chain of protrusions ascribable to the aromatic rings in the PAN molecule. Not all of the protrusions exhibited the same corrugation heights; the difference varied between 0.2 and 0.4 Å. The shortest spacing between two neighboring chains was 7 Å at 0.7 V, as compared with 10.4 Å observed for linear PAN at $E > 0.9$ V. However, we also observed a much larger spacing of $13-15$ Å between two chains, which could be necessary to accommodate the coadsorbed bisulfate anions. Indeed, close examination of the STM image in Figure 7b discloses weak yet clear protrusions lying in those wider openings. By combining the CV, XPS, and STM results, one can conclude that the conformational changes induced by the switch of potential from 0.95 to 0.7 V could arise from restructuring of the electrified PAN/Au(111) interface. At $E > 0.95$ V, the structures of PAN molecules were underpinned by regularly spaced bisulfate anions or the anchor points, and the negative shift in the potential expelled the bisulfate anions from Au(111) electrode. This act of unpinning the anchoring points thus caused twists in the PAN chains and resulted in the formation of crooked PAN.

Realignment of PAN Molecules with the Au(111) Substrate at 0.5 V. Crooked PAN molecules prevailed between 0.8 and 0.60 V. Shifting the potential negatively to 0.50 V (i.e., the negative end of peak *a* in the CV profile) triggered another major PAN conformational change back to linear again. Figure 8a−c shows high-resolution STM images acquired at 0.50 V. Chained oval protrusions arranged in zigzags are attributed to the aromatic rings in PAN molecules, as noted in Figures 5 and 7. While the crooked PAN admolecules seen in Figure 7 were arbitrarily arranged with respect to the Au(111) substrate, here the PAN molecules appeared to realign themselves with the Au(111) substrate. Two local polymeric arrays, **A** and **B**, were identified in Figure 8a, and their internal structures are shown in Figure 8b,c, respectively. The unit cells of these
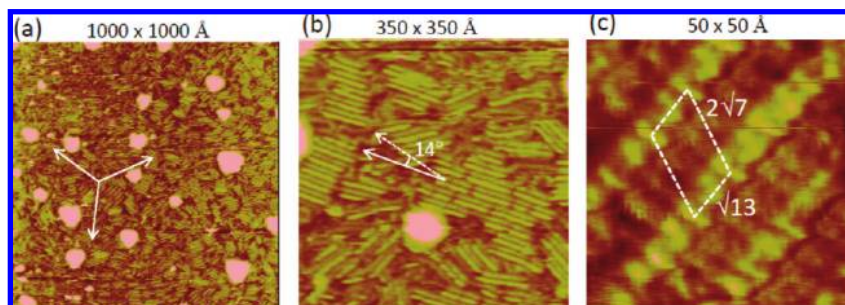
Figure 9. In situ STM images showing the structure of PAN molecules found at 0.15 V. The arrows in (a) mark the directions of the main axes of the Au(111) substrate. One of the main structures had PAN molecules misaligned with the substrate by 14°. A local structure of ($\sqrt{13} \times 2\sqrt{7}$) PAN is identified in (c).

Table 1. Summary of the Structures and Conformations of PAN Admolecules on Au(111) as a Function of Potential

potential (V)	structure	alignment of polyaniline	conformation
1.0−0.9	($3 \times 2\sqrt{3}$)	<110>	long (>300 Å) and linear
0.9−0.7	local ($3 \times 2\sqrt{3}$)	mixed	mixed
0.7−0.6	disordered	random	crooked
0.6−0.5	mixed	mixed	mixed
0.5−0.3	($3 \times 2\sqrt{3}$) + ($2\sqrt{3} \times 2\sqrt{3}$) + ($2\sqrt{3} \times \sqrt{43}$)	<121>	linear and wiggling
0.3−0.05	($\sqrt{13} \times 2\sqrt{7}$)	<110> + 14° misaligned	short (<50 Å) and linear

ordered arrays as marked are ($3 \times 2\sqrt{3}$) and ($2\sqrt{3} \times 2\sqrt{3}$) in domain **A** and ($2\sqrt{3} \times \sqrt{43}$) in domain **B**. The real-space model shown in Figure 8d accounts for the ($3 \times 2\sqrt{3}$) structure seen in domain **A**.

The formation of ordered arrays at 0.5 V is thought to result from an increase in the adsorbate−substrate interaction. While the ($3 \times 2\sqrt{3}$) and ($2\sqrt{3} \times 2\sqrt{3}$) structures consist of linear PAN chains, PAN molecules in the ($2\sqrt{3} \times \sqrt{43}$) structure are apparently wiggling. Although the reason for the formation of the wiggling molecular conformation is not known, these STM results unambiguously show that PAN molecules are rather flexible. It is now clear that the sharp peak at 0.52 V in the CV profile (Figure 1b) resulted from substantial restructuring of the PAN admolecules. In addition to the PAN molecules, in situ STM discerned weak spots embedded in the PAN chains. We attribute these features to the coadsorbed bisulfate anions, which were also identified by XPS.

The Supposedly Reduced PAN at 0.15 V. Switching the potential from 0.5 to 0.15 V yielded another major change in the PAN conformation, as revealed by the STM images shown in Figure 9. The Au(111) surface appeared to be the unreconstructed Au(111)−(1 × 1), onto which PAN molecules were adsorbed as mostly straight but short linear segments. Typically, the PANs were 50 Å in length and rarely grew to 100 Å.

PAN molecules could be aligned in several directions, but mostly they were rotated 14° from the <110> directions of the Au(111) substrate. This specific direction lays the $\sqrt{13}$ unit vector, whose length of 10.7 Å amounts to twice the spacing between two benzenoid rings in a PAN molecule. A local structure of ($\sqrt{13} \times 2\sqrt{7}$) PAN is identified in Figure 9. This result suggests that the interaction between PAN and the Au(111) substrate was still important at this potential. Although multilayer PAN was formed at 1.0 V at the beginning of the

STM imaging experiment, it could be thinned down to a monolayer thickness as the potential was shifted negatively. The alternating intensity among PAN molecules is unique and could result from different adsorption configurations, such as the adsorption sites and angle of tilting. We tried to examine this species by XPS, but unfortunately the sample was not stable toward immersion.

Finally, we summarize in Table 1 the relationship between potential and the conformation of the PAN admolecules on Au(111).

Conclusion

We have used in situ and ex situ STM, XPS, and NEXAFS to investigate the conformations of a monolayer of polyaniline molecules deposited on a Au(111) electrode in 0.1 M H_2SO_4 containing 0.03 M aniline. In situ STM revealed that aniline admolecules adsorbed in a well-ordered Au(111) ($3 \times 2\sqrt{3}$)rect structure at 0.8 V were easily oxidized and transformed into PAN molecules with a well-defined linear molecular conformation when the potential was shifted to >0.95 V. This ordered molecular array served as the template guiding the subsequent electropolymerization of aniline into a multilayer polymeric film with an interlayer spacing of 3.5 Å. This phenomenal corrugation height suggests that the PAN film, presumably in the form of the emeraldine salt at 1 V, is metallic. The chemical nature of PAN molecules remained mostly unchanged and assumed the form of the emeraldine salt between 1.0 and 0.5 V, according to the XPS results. The conformations of the emeraldine salt of PAN were altered substantially as the potential was modulated between 1.0 and 0.5 V. These potential-induced changes are associated with restructuring of the electrified interface of PAN on Au(111) and involve adsorption/desorption of bisulfate anions and PAN molecules. At 0.15 V, PAN molecules were presumed to be reduced to leucoemeraldine, giving rise to an arrangement different from that seen at 0.5 V.

Supporting Information Available: Ex situ STM image acquired with a Au(111) electrode coated with a thin film of polyaniline. This material is available free of charge via the Internet at http://pubs.acs.org.

JA809263Y